

A 10-Approximation of the $\frac{\pi}{2}$ -MST*

Ahmad Biniiaz[†] Majid Daliri[‡] Amir Hossein Moradpour[§]

Abstract

Bounded-angle spanning trees of points in the plane have received considerable attention in the context of wireless networks with directional antennas. For a point set P in the plane and an angle α , an α -spanning tree (α -ST) is a spanning tree of the complete Euclidean graph on P with the property that all edges incident to each point $p \in P$ lie in a wedge of angle α centered at p . The α -minimum spanning tree (α -MST) problem asks for an α -ST of minimum total edge length. The seminal work of Anscher and Katz (ICALP 2014) shows the NP-hardness of the α -MST problem for $\alpha = \frac{2\pi}{3}, \pi$ and presents approximation algorithms for $\alpha = \frac{\pi}{2}, \frac{2\pi}{3}, \pi$.

In this paper we study the α -MST problem for $\alpha = \frac{\pi}{2}$ which is also known to be NP-hard. We present a 10-approximation algorithm for this problem. This improves the previous best known approximation ratio of 16.

1 Introduction

Wireless antennas in a wireless network can be modeled by disks in the plane, where the centers of the disks represent locations of antennas and their radii represent transmission ranges of antennas. Two antennas can communicate if they are in each other's transmission range. In this model antennas are assumed to be omni-directional which can transmit and receive signals in 360 degrees. Replacing omni-directional antennas with *directional antennas* has received considerable attention in recent years, see for example [1, 3, 6, 8, 9, 10, 11, 13, 14, 21]. Directional antennas can transmit and receive signals only in a circular wedge with some bounded-angle α . As noted in [4, 21, 23] such a bounded-angle communication is more secure, requires lower transmission range, and causes less interference. In this model two antennas can communicate if each one is inside the other's wedge. This model is known as *symmetric communication network* [4, 5, 23].

The network connectivity is a common problem in designing networks with directional antennas. Aschner and Katz [3] formulated this problem in terms of an α -spanning tree (α -ST). For a point set P in the plane and an angle α , an α -ST of P is a spanning tree of the complete Euclidean graph on P such that all edges incident to each point $p \in P$ lie in a wedge of angle α centered at p (see Figure 1). It is known that an α -ST always exists when $\alpha \geq \frac{\pi}{3}$ (see e.g. [1, 2, 11]) while it may not exist when $\alpha < \frac{\pi}{3}$, for example if P consists of the three vertices of an equilateral triangle.

The minimum spanning tree (MST) is the shortest connected network for omni-directional antennas. For directional antennas, the shortest connected network is called the α -minimum spanning tree (α -MST) which is an α -ST of P with minimum total edge length. Although one can compute

*Appeared in the 39th International Symposium on Theoretical Aspects of Computer Science (STACS 2022).

[†]School of Computer Science, University of Windsor, ahmad.biniiaz@gmail.com, Supported by NSERC

[‡]University of Tehran, majiddl.2099@gmail.com

[§]University of Tehran, a.moradpour1378@gmail.com

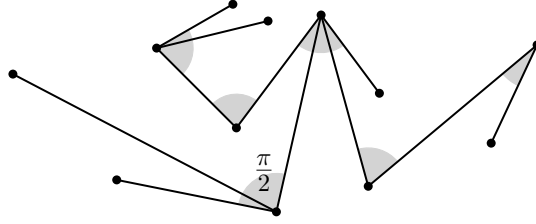


Figure 1: A $\frac{\pi}{2}$ -spanning tree.

34 an MST of n points in the plane optimally in $O(n \log n)$ time, it is not clear how to efficiently
 35 compute an α -MST. Aschner and Katz [3] proved that the α -MST problem is NP-hard for $\alpha = \frac{2\pi}{3}$
 36 and $\alpha = \pi$. They also presented approximation algorithms with ratios 16, 6, and 2 for angles
 37 $\alpha = \frac{\pi}{2}$, $\alpha = \frac{2\pi}{3}$ and $\alpha = \pi$, respectively. The approximation ratio 6 for the $\frac{2\pi}{3}$ -MST has been
 38 successively improved to 5.34 [8] and to 4 [6]. Recently Tran et al. [23] showed that the power
 39 assignment problem with directional antennas (described in Section 1.2) of angle $\frac{\pi}{2}$ is NP-hard, by
 40 a reduction from the Hamilton path problem on hexagonal grid graphs. A similar reduction can
 41 be employed to show that the $\frac{\pi}{2}$ -MST problem is also NP-hard.

42 The above approximation ratios are obtained by considering the weight of the MST as the lower
 43 bound (instead of the weight of an optimal α -MST). Of these approximation ratios, the ratio 16
 44 for $\frac{\pi}{2}$ is very interesting because for any $\alpha < \frac{\pi}{2}$ there exists a point set for which the ratio of the
 45 weight of any α -MST to the weight of any MST is $\Omega(n)$ [5]. In other words, $\alpha = \frac{\pi}{2}$ is the smallest
 46 angle for which one can obtain an α -ST of weight within some constant factor of the MST weight.
 47 However, such a factor cannot be better than 2 because for points uniformly distributed on a line
 48 the weight of α -MST could be arbitrary close to 2 times the weight of MST, for any $\alpha < \pi$ [3, 8].

49 1.1 Our contributions

50 We present an algorithm that finds a $\frac{\pi}{2}$ -ST of weight at most 10 times the MST weight (Theorem 4).
 51 Thus we obtain a 10-approximation algorithm for the $\frac{\pi}{2}$ -MST problem, improving upon the previous
 52 best known ratio of 16 due to Anscher and Katz [3]. Both our algorithm and that of [3] take linear
 53 time after computing an MST.

54 Towards obtaining the approximation ratio 10 we extend another interesting result of As-
 55 chner et al. [5] which ensures the connectivity of two sets of oriented four points that are separated
 56 by a straight line. Our extension (which is given in Theorem 2) relaxes the linear separability
 57 constraint. Most of the paper is devoted to proving this theorem.

58 1.2 Some related problems

59 There is a relationship between bounded-angle spanning trees and bounded-degree spanning trees
 60 which have received a considerable attention [7, 12, 17, 19, 20, 22]. A degree- k ST is a spanning
 61 tree in which every vertex has degree at most k . It is easily seen that any degree- k ST is an α -ST
 62 with $\alpha = 2\pi(1 - 1/k)$ because in any degree- k ST all edges that are incident to each vertex lie in
 63 some wedge of angle $2\pi(1 - 1/k)$.

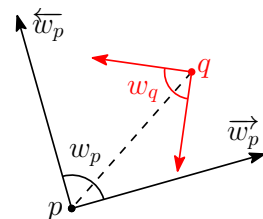
64 The α -bottleneck spanning tree (α -BST) is a closely related problem in which the goal is to
 65 compute an α -ST whose longest edge length is minimum. This problem has been studied in
 66 the context of designing networks with bounded-range directional antennas, see for example the
 67 results of Aschner et al. [3, 5] for constructing hop-spanners for unit disk graphs, Dobrev et al. [14,
 68 15] and Caragiannis et al. [10] for constructing bounded-degree strongly connected networks, and

69 Carmi et al. [11] for constructing bounded-angle Hamiltonian paths. Another related problem in
70 this context is “power assignment with directional antennas” where the objective is to assign each
71 point $p \in P$ a wedge of angle α as well as a range r_p to obtain a connected symmetric communication
72 network of minimum total power $\sum_{p \in P} (r_p)^\beta$ where $\beta \geq 1$ is the distance-power gradient [3, 5, 23].

73 Computing bounded-angle Hamiltonian paths and cycles on points in the plane is another
74 related problem. For paths it is known that any set of points in the plane admits a Hamiltonian
75 path with turning angles at most $\frac{\pi}{2}$ [11, 18] and this bound on the angle is tight [11, 16]. For cycles
76 no tight bound on the angle is known. Dumitrescu et al. [16] proved that any even-size point set
77 admits a Hamiltonian cycle with angles at most $\frac{2\pi}{3}$. The most famous conjecture in this context,
78 due to Fekete and Woeginger [18], states that any even-size point set of at least 8 elements admits
79 a Hamiltonian cycle with angles at most $\frac{\pi}{2}$.

80 1.3 Preliminaries for the algorithm

81 The following notations are adopted from [8]. Let w_p be a wedge in the
82 plane having its apex at a point p . We denote the clockwise (right) bound-
83 ary ray of w_p by \vec{w}_p and its counterclockwise (left) boundary ray by \overleftarrow{w}_p .
84 Let w_q be another wedge in the plane having its apex at a point q . If q lies
85 in w_p then we say that p sees q (or q is visible from p). We say that p and
86 q are mutually visible, denoted by $p \leftrightarrow q$, if p sees q and q sees p . In the
87 figure to the right p and q are mutually visible. Let P be a set of points in
88 the plane such that some wedge is placed at each point of P . The induced
89 mutual visibility graph of P , denoted by $G(P)$, is a geometric graph with vertex set P that has a
90 straight-line edge between two points $p, q \in P$ if and only if p and q are mutually visible. We use
91 the term “orient” to refer to placement of wedges at points. We denote the sum of edge lengths of
92 a geometric graph G by $w(G)$.



93 We define the following notations to facilitate the description of our algorithm and its analysis.
94 For two points p and q in the plane the slab $S(p, q)$ is defined as the region between two lines that
95 are perpendicular to the segment pq at points p and q (see Figure 2(a)). We use *quadruple* to
96 denote a set of four points in the plane. A quadruple Q is called *admissible* if it has two points p
97 and q such that the other two points lie in $S(p, q)$ and both on the same side of pq . In this case
98 we refer to (p, q) as an *admissible pair* of Q . Notice that a quadruple could have more than one
99 admissible pair. For a quadruple Q with a fixed admissible pair (p, q) , we define the *admissible slab*
100 of Q , denoted by $S(Q)$, to be the same as the slab $S(p, q)$; see Figure 2(a). The following lemma
101 (though very simple) plays an important role in our algorithm.

102 **Lemma 1.** *Any set P of five points in the plane contains an admissible quadruple Q such that all*
103 *points of P lie in $S(Q)$.*

104 *Proof.* Let p and q be two points that define a diameter of P , i.e., two with maximum distance. Of
105 the remaining three points of P at least two of them, say r and s , lie on the same side of $S(p, q)$.
106 Therefore $\{p, q, r, s\}$ is an admissible quadruple which we denote by Q . Since pq is a diameter of
107 P , all points of P lie in $S(p, q)$ and hence in $S(Q)$. \square

108 Our orientation of admissible quadruples in the following theorem is similar to that of Aschner,
109 Katz, and Morgenstern et al. [5] for arbitrary quadruples.

110 **Theorem 1.** *Given an admissible quadruple Q , one can place at each point of Q a wedge of angle*
111 *$\pi/2$ such that the wedges cover the plane and the induced mutual visibility graph of Q is connected.*

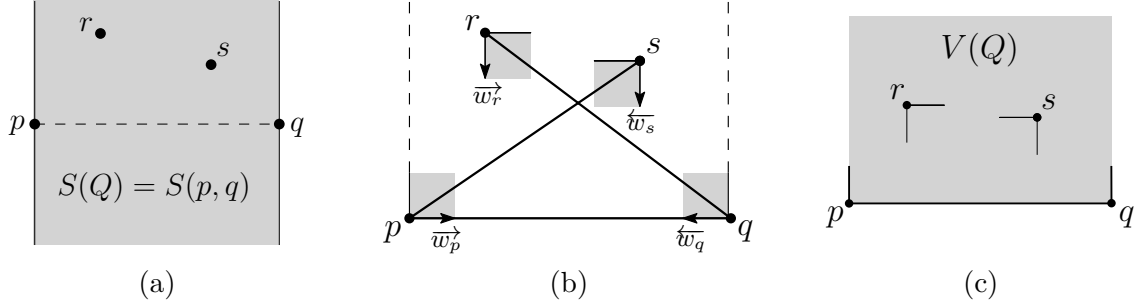


Figure 2: An admissible quadruple $Q = \{p, q, r, s\}$ with admissible pair (p, q) . Illustrations of (a) the slab $S(p, q)$ which is the same as the admissible slab $S(Q)$, (b) the proof of Theorem 1, and (c) the visibility region $V(Q)$ which is the region visible to both p and q .

112 *Proof.* Let $Q = \{p, q, r, s\}$. After a suitable relabeling, rotation and reflection assume that (p, q) is
 113 an admissible pair of Q , the line segment pq is horizontal, p is to the left of q , the points r and s
 114 lie above pq , and r is to the left of s as in Figure 2(b). We place four wedges at points of Q as in
 115 Figure 2(b). Formally, we place a wedge w_p at p such that \vec{w}_p passes through q , place w_q at q such
 116 that \vec{w}_q passes through p , place w_r at r such that q lies in w_r and \vec{w}_r is vertical, and place w_s at s
 117 such that p lies in w_s and \vec{w}_s is vertical. These four wedges cover the entire plane (if we think of the
 118 intersection point of \vec{w}_p and \vec{w}_r as the origin of the coordinate system, then the four wedges cover
 119 the four quadrants). Moreover, the induced mutual visibility graph is connected because $p \leftrightarrow q$,
 120 $r \leftrightarrow q$, and $p \leftrightarrow s$. \square

121 Recall the two points p and q in the proof of Theorem 1 that make Q admissible. Notice that
 122 after orientation of Theorem 1 the admissible slab of Q is uniquely defined by p and q . We define
 123 the *visibility region* of Q , denoted by $V(Q)$, as part of $S(Q)$ that is visible to both p and q ; see
 124 Figure 2(c) for an illustration.

125 The following theorem, which will be proved in Section 3, plays a crucial role in the correctness
 126 of our algorithm. Most of the paper is devoted to proving this theorem.

127 **Theorem 2.** *Let Q_1 and Q_2 be two admissible quadruples. Assume that wedges of angle $\pi/2$ are*
 128 *placed at points of each of Q_1 and Q_2 according to the placement in the proof of Theorem 1. Then*
 129 *at least one of the following statements holds*

- 130 (i) *The induced mutual-visibility graph of $Q_1 \cup Q_2$ is connected.*
 131 (ii) *At any point p in $S(Q_1) \cup S(Q_2)$ one can place a wedge of angle $\pi/2$ such that p is mutually*
 132 *visible from a point $q_1 \in Q_1$ and from a point $q_2 \in Q_2$. In other words the induced mutual-*
 133 *visibility graph of $Q_1 \cup Q_2 \cup \{p\}$ is connected.*

134 We note that there are admissible quadruples for which statement (i) does not hold, but (ii)
 135 holds for them; see for example Figure 9. Theorem 2 extends the following result of Aschner et al. [5]
 136 which applies only to quadruples that are separated by a line.

137 **Theorem 3** (Aschner, Katz, and Morgenstern [5], 2013). *Let Q_1 and Q_2 be two quadruples. Assume*
 138 *that wedges of angle $\pi/2$ are placed at points of each of Q_1 and Q_2 according to the placement in the*
 139 *proof of Theorem 1. If Q_1 and Q_2 are separated by a straight line, then the induced mutual-visibility*
 140 *graph of $Q_1 \cup Q_2$ is connected.*

2 The approximation algorithm

Let P be a set of n points in the plane. In this section we present our algorithm for computing a $\frac{\pi}{2}$ -ST of P of weight at most 10 times the weight of the MST of P . In Section 2.1 we describe the general framework of the algorithm. In Section 2.2 we provide the details of the algorithm and its analysis.

2.1 A general framework

Our algorithm follows the same framework as previous algorithms [3, 6, 8] which is described below. This framework was first introduced by Aschner and Katz [3].

Start by computing an MST of P . From the MST obtain a Hamiltonian path H of weight at most 2 times the weight of MST. It is well-known that such a path can be obtained by doubling the MST edges, computing an Euler tour, and then short-cutting repeated vertices. The constant 2 is tight as Fekete et al. [17] showed that for any fixed $\varepsilon > 0$ there exist point sets for which the weight of any Hamiltonian path is at least $2 - \varepsilon$ times the weight of MST.

The next step is to partition H into $\frac{n}{k}$ groups each consisting of k consecutive vertices of H for some constant k (assuming n is divisible by k). Then orient each group independently in such a way that (I) the vertices in each group are connected, and (II) there is an edge between any pair of consecutive groups. Thus the induced mutual visibility graph on P is connected. Moreover, as the vertices of the groups are connected locally (to the vertices of the same group or a neighboring group), the mutual visibility graph contains a spanning tree whose weight is within some constant factor of the weight of H . This constant depends only on k .

The original algorithms of Aschner and Katz [3] partition H into groups of size $k = 8$ for $\alpha = \frac{\pi}{2}$ and $k = 3$ for $\alpha = \frac{2\pi}{3}$. The improved algorithms of [8] and [6] (for $\alpha = \frac{2\pi}{3}$) partition H into groups of size $k = 3$ and $k = 2$, respectively.

Our algorithm partitions H into groups of size $k = 5$ for $\alpha = \frac{\pi}{2}$. The most challenging part in our algorithm (and in previous algorithms) is to maintain property (II); the proof of this property often involves detailed case analysis. There is a main difference between our algorithm and previous algorithms [3, 6, 8]. Instead of orienting all five vertices in each group simultaneously, we first *select* four of them and orient only these selected vertices. The four selected vertices form an admissible quadruple. We refer to the non-selected vertex as a *backup*. We show that, except for one “special case”, there is always a connection between two oriented admissible quadruples. For the special case we use the backup vertex to make the connection between two quadruples.

2.2 Details of our algorithm

In this section we provide details of our algorithm and its analysis. Recall that P is a set of n points in the plane, and that H is a Hamiltonian path on P such that

$$w(H) \leq 2w(\text{MST}).$$

Let h_1, \dots, h_{n-1} be the sequence of edges of H from one end to another. Partition the edges of H into five sets $H_1 = \{h_1, h_6, \dots\}$, $H_2 = \{h_2, h_7, \dots\}$, $H_3 = \{h_3, h_8, \dots\}$, $H_4 = \{h_4, h_9, \dots\}$, and $H_5 = \{h_5, h_{10}, \dots\}$. Let H_k with $k \in \{1, 2, 3, 4, 5\}$ be the edge set with the largest weight. Then

$$w(H_k) \geq \frac{w(H)}{5} \quad \text{and} \quad w(H \setminus H_k) \leq \frac{4w(H)}{5}.$$

By removing all edges of H_k from H we obtain a sequence of sub-paths each containing five vertices (except possibly the first and last sub-paths). To simplify our description we assume for

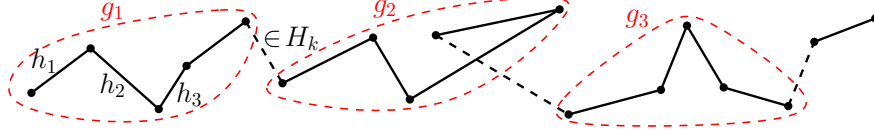


Figure 3: Illustration of the groups and sub-paths (dashed edges belong to H_k , where $k = 5$).

180 now that all sub-paths have five vertices, later in Remark 1 we will take care of the case where the
 181 first and last sub-paths have less than five vertices. We refer to the five vertices of each sub-path as
 182 a *group*. Let g_1, g_2, \dots, g_m denote the sequence of the groups that is corresponding to the sequence
 183 of sub-paths along H as in Figure 3.

184 From each group g_i we take an admissible quadruple Q_i (consisting of four vertices) as in the
 185 proof of Lemma 1. We denote the remaining vertex of g_i by b_i ; this is a backup vertex. By Lemma 1,
 186 b_i lies in $S(Q_i)$. We orient each admissible quadruple Q_i according to the orientation in the proof of
 187 Theorem 1 which ensures the connectivity of the induced mutual visibility graph $G(Q_i)$. Consider
 188 any two consecutive oriented quadruples Q_i and Q_{i+1} . By Theorem 2 at least one of the following
 189 statements holds:

- 190 (i) The graph $G(Q_i \cup Q_{i+1})$ is connected, i.e., there is an edge between Q_i and Q_{i+1} .
 191 (ii) Any point p in $S(Q_i) \cup S(Q_{i+1})$ can be oriented so that $G(Q_i \cup Q_{i+1} \cup \{p\})$ is connected.

192 If statement (i) holds then we orient b_i towards a vertex of Q_i that sees b_i (such a vertex exists
 193 because the orientation of Theorem 1 covers the entire plane). If (i) does not hold but (ii) holds
 194 then we orient b_i in such a way that it connects Q_i and Q_{i+1} .

195 To this end all vertices are oriented except the backup vertex b_m of g_m . We orient b_m towards
 196 a vertex of Q_m that sees b_m . Thus, we obtain a connected induced mutual visibility graph $G(P)$.

197 Now we obtain a spanning tree T of $G(P)$ as follows: First we take an arbitrary spanning tree T_i
 198 from each $G(Q_i)$. Then we connect each pair T_i and T_{i+1} either by a direct edge (if (i) holds) or via
 199 a backup vertex (if (ii) holds). Lastly we connect any remaining backup vertex to its corresponding
 200 quadruple by an edge. This gives a spanning tree T that we report as the output of our algorithm.
 201 Notice that the trees T_i are not necessarily minimum spanning trees of graphs $G(Q_i)$; we will use
 202 the triangle inequality to bound the length of T .

203 **Analysis of the approximation ratio.** To bound the weight of T , we charge the edges of H
 204 for the edges of T as follows. By the triangle inequality, the weight of every edge (p, q) of T is at
 205 most the weight of the unique path in H between p and q . We charge the weight of the edges of
 206 this path for the edge (p, q) . Every edge of H_k is charged only once and that is for connecting two
 207 consecutive trees T_i and T_{i+1} (either directly or via a backup vertex). Every edge of $H \setminus H_k$ (i.e.,
 208 every edge of each sub-path) is charged at most six times: three times for the three edges of T_i ,
 209 two times for the two edges connecting T_i to T_{i+1} and to T_{i-1} , and once for the edge connecting
 210 the backup vertex b_i to T_i . Therefore

$$\begin{aligned} w(T) &\leq w(H_k) + 6w(H \setminus H_k) \\ &= w(H) + 5w(H \setminus H_k) \leq w(H) + 5 \cdot \frac{4w(H)}{5} = 5w(H) \leq 10w(\text{MST}). \end{aligned}$$

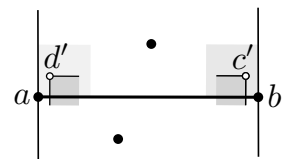
211 **Running-time analysis.** After computing an MST in $O(n \log n)$ time, the rest of the algorithm

212 (computing H , finding H_k , orienting admissible quadruples and backup vertices, and obtaining T)
 213 takes $O(n)$ time.

214 **Remark 1.** Here we handle the case where the first sub-path, denoted by δ , has less than five
 215 vertices (the last sub-path will be treated analogously). This case is essentially a simple version of
 216 Theorem 2 where fewer points are involved. We will use Theorem 2 to handle this case, however it
 217 could also be handled directly but with some case analysis.

218 We will connect the vertices of δ to g_1 (the first 5-vertex group). Let Q be g_1 's admissible
 219 quadruple. Since the oriented points in Q cover the entire plane, it might be tempting to orient
 220 each point p of δ towards the point of Q that sees p . This approach may not be suitable when δ has
 221 more than one point because to maintain the ratio 10 we should not connect Q to its preceding
 222 group (here to δ) by more than one edge. To remedy this, we use our Theorem 2.

223 As discussed above, we may assume that δ has 2, 3, or 4 points. Let
 224 ab be a diameter of δ . Thus, δ has points a , b , and at most two other
 225 “real” points. We place a “fake” point c' in $S(a, b)$ and very close to b
 226 such that both c' and b lie on the same side of any line through boundary
 227 rays of wedges in Q . In the same fashion we place a fake point d' very
 228 close to a , and on the same side of ab as c' . Let $Q' = \{a, b, c', d'\}$. Our
 229 placement of c' and d' —in $S(a, b)$ and on the same side of ab —implies that Q' is an admissible
 230 quadruple with admissible pair (a, b) . We orient Q' according to Theorem 1. By Theorem 2-part
 231 (i), a point of Q' and a point of Q are mutually visible (our placement of c' and d' together with
 232 Property 1 from the next section imply that part (i) of Theorem 2 holds). If the visibility is through
 233 a real point say b , then we reflect the orientation of a with respect to ab . After reflection, a and
 234 b remain mutually visible, and their wedges cover the entire region $S(a, b)$. Then we orient every
 235 other real vertex of δ towards the one of a and b that sees it. If the visibility is through a fake
 236 point say c' then the point of Q , say q , that sees c' also sees b (this is implied by our placement of
 237 c'). In this case we reflect the orientation of b with respect to ab so that b is mutually visible with
 238 q , and a and b together see the entire region $S(a, b)$. Then we orient every other real vertex of δ
 239 towards the one of a and b that sees it. In either case we remove fake points. Therefore the mutual
 240 visibility graph on points of δ is connected, and it has a connection to a point in Q via a or b .



241 The following theorem summarizes our main result.

242 **Theorem 4.** For any set of points in the plane and any angle $\alpha \geq \frac{\pi}{2}$, there is an α -spanning tree
 243 of length at most 10 times the length of the MST. Furthermore, there is an algorithm that finds
 244 such an α -spanning tree in linear time after construction of the MST.

245 3 Proof of Theorem 2

246 In this section we prove Theorem 2 which says: Let Q_1 and Q_2 be two admissible quadruples.
 247 Assume that wedges of angle $\pi/2$ are placed at points of each of Q_1 and Q_2 according to the
 248 placement in the proof of Theorem 1. Then at least one of the following statements holds

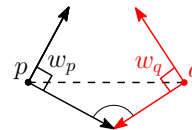
- 249 (i) The induced mutual-visibility graph of $Q_1 \cup Q_2$ is connected.
- 250 (ii) At any point p in $S(Q_1) \cup S(Q_2)$ we can place a wedge of angle $\pi/2$ such that p is mutually
 251 visible from a point $q_1 \in Q_1$ and from a point $q_2 \in Q_2$. In other words the induced mutual-
 252 visibility graph of $Q_1 \cup Q_2 \cup \{p\}$ is connected.

253 Our proof is involved. For a better understanding we split our proof into smaller pieces based on
 254 the relative position of admissible pairs of Q_1 and Q_2 . Let $Q_1 = \{a, b, c, d\}$ and $Q_2 = \{a', b', c', d'\}$.
 255 After a suitable relabeling assume that (a, b) and (a', b') are the admissible pairs of Q_1 and Q_2 ,
 256 respectively, that are considered in the orientation of Theorem 1. Also assume that—after the
 257 orientation of Theorem 1— c looks towards a while d looks towards b , and similarly c' looks towards
 258 a' while d' looks towards b' as in Figures 4-10. We use this notation throughout our proof without
 259 further mentioning. Up to symmetry we have the following four cases:

- 260 A. $a'b'$ intersects ab .
- 261 B. The extension of $a'b'$ intersects the extension of ab .
- 262 C. The extension of $a'b'$ intersects ab .
- 263 D. $a'b'$ is parallel to ab .

264 After a suitable rotation we assume that ab is horizontal and a is to the left of b . We denote
 265 by ℓ the line through ab and by ℓ' the line through $a'b'$ as in Figure 4(a). For a point x we denote
 266 by ℓ_x the line through x that is perpendicular to ℓ , and denote by ℓ'_x the line through x that is
 267 perpendicular to ℓ' . For a line l in the plane we use the terms “above” and “below” to refer to the
 268 two half planes on the two sides of l . If l is vertical then “below” refers to the left-side half plane
 269 and “above” refers to the right-side half plane. Throughout our proof, we use the following obvious
 270 observation about mutual visibility without mentioning it in all occurrences.

Observation 1. Assume that wedges w_p and w_q of angles $\frac{\pi}{2}$ are placed at two points p and q . If the clockwise (resp. counterclockwise) boundary ray of w_p meets the counterclockwise (resp. clockwise) boundary ray of w_q at an obtuse or a right angle then p and q are mutually visible.



271
 272
 273 Some part of our proof (where Q_1 and Q_2 are separated by a line) could be implied from
 274 Theorem 3. However, for the sake of completeness we provide our own proof. We provide the proof
 275 of the first cases, A and B-1, with more formal details. To simplify our description, we will refer
 276 to the clockwise (resp. counterclockwise) boundary ray of the wedge that is placed at a point p by
 277 “the clockwise (resp. counterclockwise) ray of p ”.

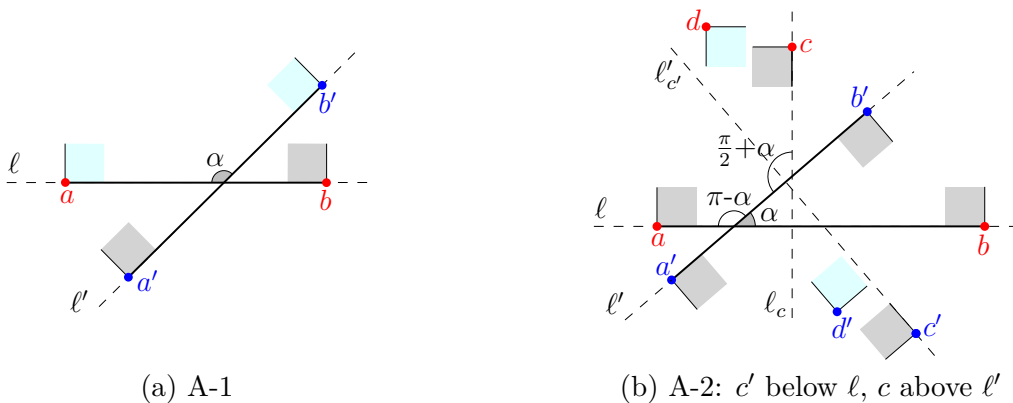


Figure 4: Illustration of the proof of case A.

278 **A. $a'b'$ intersects ab**

279 We denote by α the intersection angle of ab and $a'b'$ that lies in $V(Q_1) \cap V(Q_2)$. We say that α is
 280 *defined* by the two vertices that lie on this angle. For example in Figure 4(a) the angle α is defined
 281 by a and b' . Depending on the value of α we consider the following two cases.

- 282 1. $\alpha \geq \frac{\pi}{2}$. After a suitable relabeling we assume that α is defined by a and b' , as in Figure 4(a).
 283 In this case the clockwise ray of a and the counterclockwise ray of b' meet at angle α , and
 284 thus a and b' are mutually visible by Observation 1.
- 285 2. $\alpha < \frac{\pi}{2}$. After a suitable relabeling we assume that α is defined by b and b' , as in Figure 4(b).
 286 If c' is above ℓ then the clockwise ray of a and the counterclockwise ray of c' meet at angle
 287 $\pi - \alpha$, and thus c' and a are mutually visible by Observation 1. Similarly if c is below ℓ' then
 288 c and a' are mutually visible. Assume that c' is below ℓ and c is above ℓ' as in Figure 4(b).
 289 If d' is to the left of ℓ_c then the clockwise ray of d' and the counterclockwise ray of c meet at
 290 angle $\frac{\pi}{2} + \alpha$, and thus d' and c are mutually visible by Observation 1. Similarly if d is below
 291 ℓ'_c then d and c' are mutually visible. Assume that d' is to the right of ℓ_c , and d is above
 292 ℓ'_c . In this setting which is depicted in Figure 4(b), d and d' lie in opposite cones formed by
 293 intersection of ℓ_c and ℓ'_c , and thus d and d' are mutually visible (observe that the clockwise
 294 ray of d and the counterclockwise ray of d' meet at angle $\pi - \alpha$).

295 **B. The extension of $a'b'$ intersects the extension of ab**

296 Let α be the angle at which the extensions of ab and $a'b'$ meet each other as in Figures 5 and 6.
 297 After a suitable reflection and relabeling we assume that $a'b'$ lies below ℓ , their extensions meet
 298 at a point m to the right of b , and a' is farther from m than b' . Depending on the value of α we
 299 consider two cases.

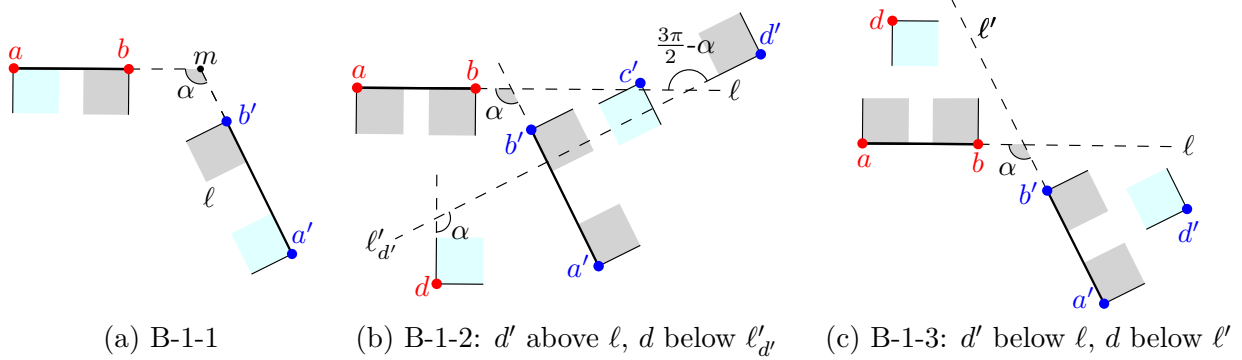


Figure 5: Illustration of the proof of case B-1.

- 300 1. $\alpha \geq \frac{\pi}{2}$. Depending on visibility regions of Q_1 and Q_2 we consider three sub-cases (up to
 301 symmetry).
 - 302 1. $V(Q_1)$ lies below ab and $V(Q_2)$ lies below $a'b'$ as in Figure 5(a). In this case the clockwise
 303 ray of a' and the counterclockwise ray of a meet at angle α , and hence $a \leftrightarrow a'$ by
 304 Observation 1.
 - 305 2. $V(Q_1)$ lies below ab and $V(Q_2)$ lies above $a'b'$. See Figure 5(b). If d' is below ℓ then
 306 the clockwise ray of d' and the counterclockwise ray of a meet at angle α and hence

307
308
309
310
311
312
313
314

$a \leftrightarrow d'$. Assume that d' is above ℓ . If d is above $\ell'_{a'}$ then the clockwise ray of d and the counterclockwise ray of d' meet at angle $\frac{3\pi}{2} - \alpha$ and thus $d \leftrightarrow d'$. Assume that d is below $\ell'_{a'}$. In this setting which is depicted in Figure 5(b) the clockwise ray of c' and the counterclockwise ray of d meet at angle α and thus $c' \leftrightarrow d$.

3. $V(Q_1)$ lies above ab and $V(Q_2)$ lies above $a'b'$. See Figure 5(c). If d' is above ℓ then $a \leftrightarrow d'$. Similarly if d is above ℓ' then $a' \leftrightarrow d$. Assume that d' is below ℓ and d is below ℓ' . In this setting which is depicted in Figure 5(c) the clockwise ray of d' and the counterclockwise ray of d meet at angle α and thus $d \leftrightarrow d'$.

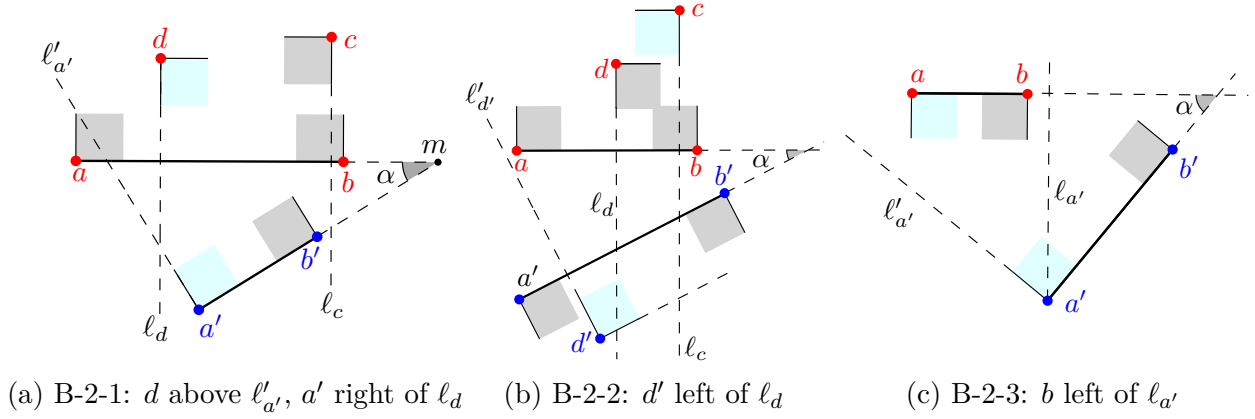


Figure 6: Illustration of the proof of case B-2.

315
316
317
318
319
320
321
322
323
324
325
326
327

2. $\alpha < \frac{\pi}{2}$. Similar to the previous case here we also consider three sub-cases.

1. $V(Q_1)$ lies above ab and $V(Q_2)$ lies above $a'b'$. See Figure 6(a). If d is below $\ell'_{a'}$ then d and b' are mutually visible. If a' is to the left of ℓ_d then a' and c are mutually visible. Assume that d is above $\ell'_{a'}$ and a' is to the right of ℓ_d as in Figure 6(a). In this setting d and a' are mutually visible.
2. $V(Q_1)$ lies above ab and $V(Q_2)$ lies below $a'b'$. If d' is to the left of ℓ_d then $c \leftrightarrow d'$ as in Figure 6(b). Analogously if d is below $\ell'_{a'}$ then $c' \leftrightarrow d$. Therefore assume that d' is to the right of ℓ_d and d is above $\ell'_{a'}$. In this setting $d \leftrightarrow d'$.
3. $V(Q_1)$ lies below ab and $V(Q_2)$ lies above $a'b'$. See Figure 6(c). Consider $\ell_{a'}$, i.e., the line through a' that is perpendicular to ℓ . If b is to the right of $\ell_{a'}$ then $a' \leftrightarrow b$. Assume that b is to the left of $\ell_{a'}$ as in Figure 6(c). Now we look at $\ell'_{a'}$. If a is above this line then $a \leftrightarrow a'$, otherwise $a \leftrightarrow b'$. (Notice that when a is above $\ell'_{a'}$ then a and b' may not be mutually visible, for example when b' is very close to a' .)

328 C. The extension of $a'b'$ intersects ab

329 We denote by m the intersection point of ℓ' and ab . After a suitable reflection and relabeling we
330 assume that $a'b'$ lies below ℓ , a' is farther from m than b' , and angle $\angle a'ma \leq \frac{\pi}{2}$, as in Figure 7.
331 Depending on visibility regions of Q_1 and Q_2 we consider four cases.

- 332 1. $V(Q_1)$ lies below ab and $V(Q_2)$ lies below $a'b'$ as in Figure 7(a). In this case $a' \leftrightarrow b$.
- 333 2. $V(Q_1)$ lies above ab and $V(Q_2)$ lies above $a'b'$. If c is to the left of $\ell_{a'}$ then so is d , as in
334 Figure 7(b). In this case d sees both a' and b' , and at least one of a' and b' sees d , and thus

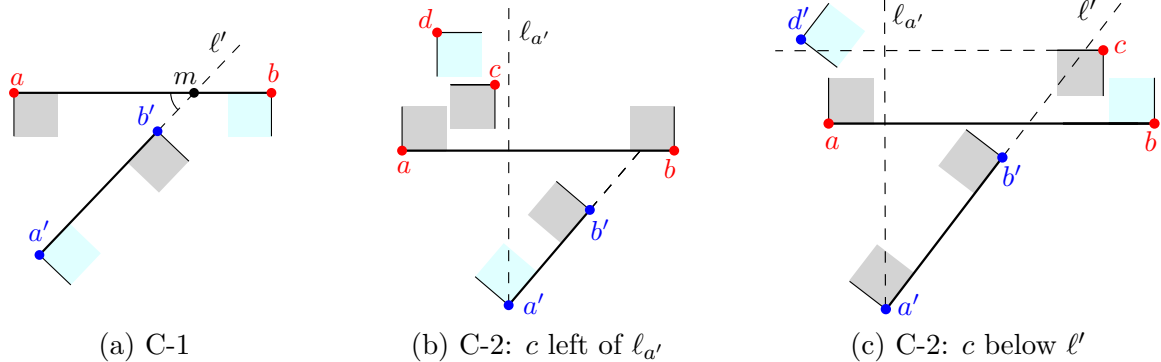


Figure 7: Illustration of the proof of cases C-1 and C-2.

335 $d \leftrightarrow a'$ or $d \leftrightarrow b'$. Assume that c is to the right of $l_{a'}$. If c is above l' then $c \leftrightarrow a'$. Thus,
 336 assume that c is below l' as in Figure 7(c). Recall that d' is in slab $S(a', b')$. If d' is above
 337 the horizontal line through c then $d' \leftrightarrow b$, otherwise $d' \leftrightarrow c$.

338 3. $V(Q_1)$ lies above ab and $V(Q_2)$ lies below $a'b'$. This case is depicted in Figure 8. If c is below
 339 l' then $c \leftrightarrow a'$. Assume that c is above l' . If d' is to the left of l_c then $c \leftrightarrow d'$ as in Figure 8(a).
 340 Assume that d' is to the right of l_c (and hence to the right of l_d). Now we look at d with
 341 respect to $l'_{d'}$. If d is above $l'_{d'}$ then $d \leftrightarrow d'$. If d is below $l'_{d'}$ then it is also below $l'_{c'}$ and thus
 342 $d \leftrightarrow c'$ as in Figure 8(b).

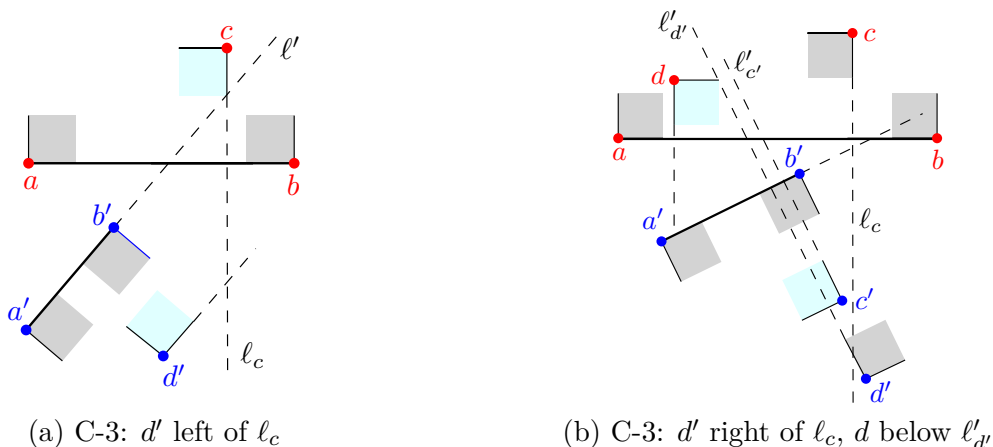


Figure 8: Illustration of the proof of case C-3.

343 4. $V(Q_1)$ lies below ab and $V(Q_2)$ lies above $a'b'$. This case is depicted in Figure 9. If d' is
 344 below l then $d' \leftrightarrow b$. Assume that d' is above l . If a is below $l'_{b'}$ then $a \leftrightarrow b'$. Assume that
 345 a is above $l'_{b'}$. If c is above $l'_{d'}$ then $c \leftrightarrow d'$. Assume that c is below $l'_{d'}$ (which is also below
 346 $l'_{c'}$). Notice that c' lies in the slab bounded by $l'_{b'}$ and $l'_{d'}$. If c' is to the left of l_c then $c' \leftrightarrow c$.
 347 Assume that c' is to the right of l_c . Notice that d lies in the vertical slab bounded by l_a and
 348 l_c . Let l_1 be the line through c' parallel to l' . If d is below l_1 then $d \leftrightarrow c'$. Assume that d
 349 is above l_1 . This configuration is depicted in Figure 9 (the caption of this figure summarizes
 350 the constraints). This is the configuration for which statement (i) of the theorem does not
 351 hold; for all other configurations statement (i) holds. We will show that statement (ii) holds
 352 in the current setting.

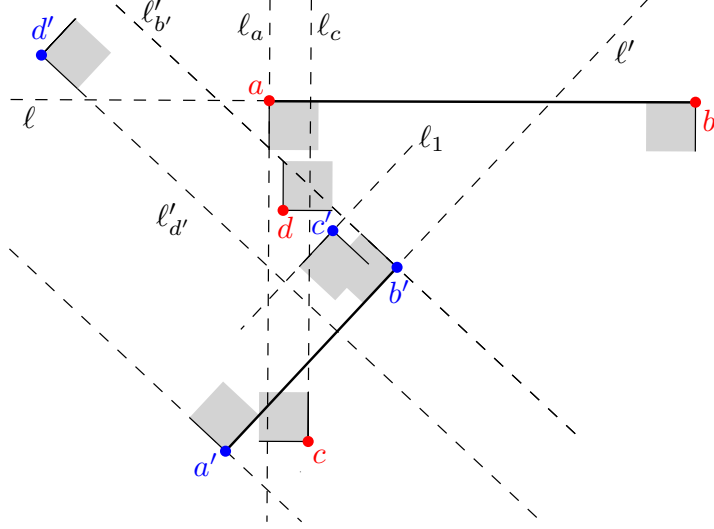


Figure 9: Illustration of case C-4: d' is above ℓ , a is above $\ell'_{b'}$, c is below $\ell'_{d'}$, c' is to the right of ℓ_c (and in the slab defined by $\ell'_{d'}$ and $\ell'_{b'}$), and d is above ℓ_1 (and in the slab defined by ℓ_a and ℓ_c). In this figure, Q_1 and Q_2 are oriented according to Theorem 1 but there is no mutual visibility between points of Q_1 and points of Q_2 (statement (i) in Theorem 2 does not hold here).

353 First, we extract a property of the current setting which is used in Remark 1. See Figure 9
 354 for a better understanding of this property, and notice that in the current setting the points
 355 b, c lie on different sides of $\ell'_{b'}$, and the points a', d' lie on different sides of ℓ .

356 **Property 1.** *If statement (i) in Theorem 2 does not hold then then the points b, c or the*
 357 *points a, d of Q_1 lie on different sides of a line through boundary rays of wedges of Q_2 , and*
 358 *similarly the points b', c' or the points a', d' of Q_2 lie on different sides of a line through*
 359 *boundary rays of wedges of Q_1 .*

360 To verify that statement (ii) holds in the current setting, let p be any point in the region
 361 $S(Q_1) \cup S(Q_2)$. We show how to place a wedge of angle $\frac{\pi}{2}$ at p so that p is mutually visible
 362 from a point in Q_1 and a point in Q_2 . To simplify our description we partition $S(Q_1) \cup S(Q_2)$
 363 into eight regions R_1, \dots, R_8 as in Figure 10. If $p \in R_1$ then we orient p similar to d' , and
 364 thus $p \leftrightarrow b$ and $p \leftrightarrow b'$. If $p \in R_2$ then we orient p similar to a , and thus $p \leftrightarrow c$ and $p \leftrightarrow b'$. If
 365 $p \in R_3$ then we orient it similar to c' so that $p \leftrightarrow c$ and $p \leftrightarrow a'$. If $p \in R_4$ then we orient it
 366 similar to b so that $p \leftrightarrow d$ and $p \leftrightarrow a'$. If $p \in R_5$ then we orient it similar to b' , and hence $p \leftrightarrow d$
 367 and $p \leftrightarrow d'$. If $p \in R_6$ then we orient it similar to c , and thus $p \leftrightarrow a$ and $p \leftrightarrow d'$. If $p \in R_7$ then
 368 we orient it similar to a' so that $p \leftrightarrow a$ and $p \leftrightarrow c'$. Finally if $p \in R_8$ then we orient it similar
 369 to d , and hence $p \leftrightarrow b$ and $p \leftrightarrow c'$. Thus statement (ii) of the theorem holds.

370 D. $a'b'$ is parallel to ab

371 Assume that ab and $a'b'$ are horizontal, and ab lies above $a'b'$. Consider any horizontal line h
 372 between ab and $a'b'$. One pair of points from Q_1 (either (a, b) or (c, d)) covers the half plane below
 373 h . Also, one pair of points from Q_2 (either (a', b') or (c', d')) covers the half plane above h . One can
 374 simply verify that there is an edge between these two pairs in the induced mutual visibility graph.

375 This is the end of our proof of Theorem 2.

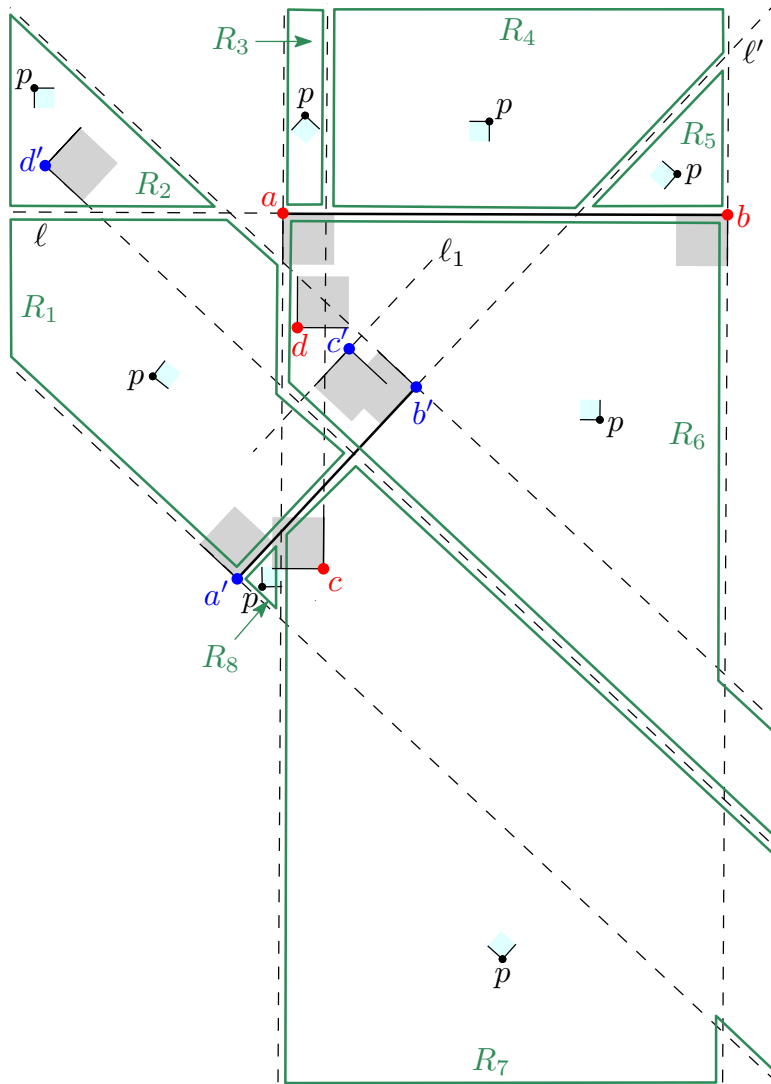


Figure 10: Partitioning $S(Q_1) \cup S(Q_2)$ into regions R_1, \dots, R_8 .

4 Conclusions

The obvious open problem is to improve our approximation ratio 10 which we think is not the best possible ratio. The use of a Hamiltonian path is a bottleneck towards our analysis as it forces a factor of 2 in the ratio. It might be possible to get better ratios by using the original MST instead of the path. Perhaps the MST may not be the best lower bound either because one may obtain a better ratio by considering the $\frac{\pi}{2}$ -MST as a lower bound.

References

- [1] E. Ackerman, T. Glander, and R. Pinchasi. Ice-creams and wedge graphs. *Computational Geometry: Theory and Applications*, 46(3):213–218, 2013.
- [2] O. Aichholzer, T. Hackl, M. Hoffmann, C. Huemer, A. Pór, F. Santos, B. Speckmann, and B. Vogtenhuber. Maximizing maximal angles for plane straight-line graphs. *Computational*

- 387 *Geometry: Theory and Applications*, 46(1):17–28, 2013. Also in *WADS’07*.
- 388 [3] R. Aschner and M. J. Katz. Bounded-angle spanning tree: Modeling networks with angular
389 constraints. *Algorithmica*, 77(2):349–373, 2017. Also in *ICALP’14*.
- 390 [4] R. Aschner, M. J. Katz, and G. Morgenstern. Do directional antennas facilitate in reducing in-
391 terferences? In *Proceedings of the 13th Scandinavian Symposium and Workshops on Algorithm
392 Theory (SWAT)*, pages 201–212, 2012.
- 393 [5] R. Aschner, M. J. Katz, and G. Morgenstern. Symmetric connectivity with directional an-
394 tennas. *Computational Geometry: Theory and Applications*, 46(9):1017–1026, 2013. Also in
395 *ALGOSENSORS’12*.
- 396 [6] S. Ashur and M. J. Katz. A 4-approximation of the $\frac{2\pi}{3}$ -MST. In *Proceedings of the 17th
397 Algorithms and Data Structures Symposium (WADS)*, 2021.
- 398 [7] A. Biniáz. Euclidean bottleneck bounded-degree spanning tree ratios. *Discrete & Computa-
399 tional Geometry*, <https://doi.org/10.1007/s00454-021-00286-4>, 2021. Also in *SODA’20*.
- 400 [8] A. Biniáz, P. Bose, A. Lubiw, and A. Maheshwari. Bounded-Angle Minimum Spanning Trees.
401 In *Proceedings of the 17th Scandinavian Symposium and Workshops on Algorithm Theory
402 (SWAT 2020)*, pages 14:1–14:22, 2020.
- 403 [9] P. Bose, P. Carmi, M. Damian, R. Y. Flatland, M. J. Katz, and A. Maheshwari. Switch-
404 ing to directional antennas with constant increase in radius and hop distance. *Algorithmica*,
405 69(2):397–409, 2014. Also in *WADS’11*.
- 406 [10] I. Caragiannis, C. Kaklamanis, E. Kranakis, D. Krizanc, and A. Wiese. Communication in
407 wireless networks with directional antennas. In *Proceedings of the 20th Annual ACM Sympo-
408 sium on Parallelism in Algorithms and Architectures (SPAA)*, pages 344–351, 2008.
- 409 [11] P. Carmi, M. J. Katz, Z. Lotker, and A. Rosén. Connectivity guarantees for wireless networks
410 with directional antennas. *Computational Geometry: Theory and Applications*, 44(9):477–485,
411 2011.
- 412 [12] T. M. Chan. Euclidean bounded-degree spanning tree ratios. *Discrete & Computational
413 Geometry*, 32(2):177–194, 2004. Also in *SoCG’03*.
- 414 [13] M. Damian and R. Y. Flatland. Spanning properties of graphs induced by directional antennas.
415 *Discrete Mathematics, Algorithms and Applications*, 5(3), 2013.
- 416 [14] S. Dobrev, E. Kranakis, D. Krizanc, J. Opatrny, O. M. Ponce, and L. Stacho. Strong connec-
417 tivity in sensor networks with given number of directional antennae of bounded angle. *Discrete
418 Mathematics, Algorithms and Applications*, 4(3), 2012. Also in *COCOA’10*.
- 419 [15] S. Dobrev, E. Kranakis, O. M. Ponce, and M. Plzík. Robust sensor range for constructing
420 strongly connected spanning digraphs in UDGs. In *Proceedings of the 7th International Com-
421 puter Science Symposium in Russia (CSR)*, pages 112–124, 2012.
- 422 [16] A. Dumitrescu, J. Pach, and G. Tóth. Drawing Hamiltonian cycles with no large angles.
423 *Electronic Journal of Combinatorics*, 19(2):P31, 2012. Also in *GD’94*.

- 424 [17] S. P. Fekete, S. Khuller, M. Klemmstein, B. Raghavachari, and N. E. Young. A network-
425 flow technique for finding low-weight bounded-degree spanning trees. *Journal of Algorithms*,
426 24(2):310–324, 1997. Also in *IPCO* 1996.
- 427 [18] S. P. Fekete and G. J. Woeginger. Angle-restricted tours in the plane. *Computational Geometry:*
428 *Theory and Applications*, 8:195–218, 1997.
- 429 [19] R. Jothi and B. Raghavachari. Degree-bounded minimum spanning trees. *Discrete Applied*
430 *Mathematics*, 157(5):960–970, 2009.
- 431 [20] S. Khuller, B. Raghavachari, and N. E. Young. Low-degree spanning trees of small weight.
432 *SIAM Journal on Computing*, 25(2):355–368, 1996. Also in *STOC'94*.
- 433 [21] E. Kranakis, F. MacQuarrie, and O. M. Ponce. Connectivity and stretch factor trade-offs in
434 wireless sensor networks with directional antennae. *Theoretical Computer Science*, 590:55–72,
435 2015.
- 436 [22] C. L. Monma and S. Suri. Transitions in geometric minimum spanning trees. *Discrete &*
437 *Computational Geometry*, 8:265–293, 1992. Also in *SoCG'91*.
- 438 [23] T. Tran, M. K. An, and D. T. Huynh. Antenna orientation and range assignment algorithms
439 in directional WSNs. *IEEE/ACM Transaction on Networking*, 25(6):3368–3381, 2017. Also in
440 *INFOCOM'16*.